Earth's Future

RESEARCH ARTICLE
10.1029/2024EF004505

Intensification and Changing Spatial Extent of Heavy Rainfall in Urban Areas

Herminia Torelló-Sentelles[1], Francesco Marra[2,3], Marika Koukoula[1], Gabriele Villarini[4,5], and Nadav Peleg[1]

[1]Institute of Earth Surface Dynamics, University of Lausanne, Lausanne, Switzerland, [2]Department of Geosciences, University of Padova, Padova, Italy, [3]Institute of Atmospheric Sciences and Climate, National Research Council (CNR-ISAC), Bologna, Italy, [4]Department of Civil and Environmental Engineering, Princeton University, Princeton, NJ, USA, [5]High Meadows Environmental Institute, Princeton University, Princeton, NJ, USA

Key Points:

- Heavy rainfall is intensified over urban areas and the effect is related to city size
- Urban areas usually alter rainfall spatial structure by increasing its spatial heterogeneity and reducing its area
- There are increased storm initiations over most urban areas in the late afternoon and evening hours

Supporting Information:

Supporting Information may be found in the online version of this article.

Correspondence to:

H. Torelló-Sentelles,
herminia.torello@unil.ch

Citation:

Torelló-Sentelles, H., Marra, F., Koukoula, M., Villarini, G., & Peleg, N. (2024). Intensification and changing spatial extent of heavy rainfall in urban areas. *Earth's Future*, *12*, e2024EF004505. https://doi.org/10.1029/2024EF004505

Received 2 FEB 2024
Accepted 2 AUG 2024

Abstract Urban areas have been shown to impact rainfall by altering both its intensity and spatial structure at sub-hourly and sub-kilometer scales. However, there is currently no clear understanding of the precise pattern of change and the mechanisms that drive these changes. Since the hydrological response in urban areas is highly sensitive to such rainfall properties, understanding these changes is critical to improving our ability to assess urban flood risk. We use 7 years of high-resolution weather radar data (4- or 5-min and 1 km) to analyze changes in patterns of rainfall intensity, spatial structure, and storm evolution across eight urban areas within Europe and the United States. The use of the same methodology across the different cities enables a consistent comparison among them. We track convective rainfall events using a storm tracking algorithm and assess changes in rainfall properties in the upwind, center, and downwind regions of each city. We also investigate changes in the frequency of storm initiations, terminations, splitting, and merging. Our results show that urban areas act to intensify rainfall—mostly over them, but sometimes on their peripheries. Overall, larger cities tend to show the largest rainfall enhancements. Our findings highlight that rainfall spatial structure is altered over the urban core; usually resulting in more spatially concentrated rainfall. We also observe increased storm initiations over most cities and increased storm splitting over one. Given that demographic projections show that future urban population will increase, our results point toward an increased future flood risk in growing cities.

Plain Language Summary Urban flood risk is highly sensitive to the intensity and patterns of precipitation. At the same time, urban areas have been shown to impact rainfall by altering these properties. It is important to improve our understanding of how rainfall is modified by cities to better anticipate future flood risk. Here, we use weather radar observations to analyze changes in rainfall intensity and patterns across eight urban areas within Europe and the United States. Our results show that rainfall becomes more intense over cities compared to their surroundings, and sometimes on the city edges. Larger cities show larger increases in intensity. Our findings also show that rainfall usually becomes more spatially concentrated when passing the cities. Finally, we observe that more storms emerge over the cities in comparison to their surroundings, mostly in the late afternoon to evening hours. Given that we expect that cities will become larger and denser in the future, our results indicate that future flood risk may also increase in growing cities as urban rainfall trends toward increasing extremes.

1. Introduction

Urban areas are becoming larger and more populated. As of 2018, over half of the world's population is living in urban areas and this has been projected to increase to 68% by 2050 (UN-DESA, 2018). To accommodate for this, urban areas are expanding and their form is also changing (Marshall, 2007; Seto et al., 2010). Urban development results in land use changes that increase flood risk, mainly because the permeability of the land surface is reduced (Jha et al., 2012). At the same time, short-duration rainfall events caused by convection, which are the most relevant for urban flooding, are expected to intensify with global warming (Seneviratne et al., 2021; Westra et al., 2014). It is also anticipated that heavy rainfall will intensify in the urban environment, but the complexity of the system makes it particularly difficult to accurately estimate the city effects (Han et al., 2014). Thus, flood risk is expected to increase in cities due to this increased exposure and hazard. To reduce urban flood hazards, and make future cities more flood-sustainable, there is a need to first understand how extreme rainfall events are modified due to the urban environment and then suggest ways to improve the urban drainage systems.

The main hypothesized mechanisms behind urban rainfall modification fall into three main categories: changes to thermodynamic, dynamic, and microphysical processes (Oke et al., 2017). In the first case, the urban heat island (UHI) effect destabilizes the boundary layer and induces thermally driven circulations which cause low-level convergence and convection (Han & Baik, 2008; Lin & Smith, 1986; Olfe & Lee, 1971). In addition, urban areas may also alter the availability of moisture in the urban boundary layer (Mölders & Olson, 2004; Shepherd, 2006). Secondly, urban surface roughness can modify airflow near and over urban areas. This may slow down near-surface winds over cities, causing convergence and upward motion upwind and over them, and divergence and downward motion downwind of them (Oke et al., 2017). Thirdly, increased urban aerosol concentrations can suppress or enhance precipitation. Aerosols can suppress precipitation by absorbing and reflecting solar radiation, which leads to the heating of the atmosphere (Haywood & Boucher, 2000; Ramanathan et al., 2001), or, by increasing the concentration of cloud condensation nuclei which can increase the number of small cloud drops nucleated and slow down the conversion of cloud water to rainfall (Han et al., 2014; Haywood & Boucher, 2000; Rosenfeld et al., 2008). Increased concentration of cloud condensation nuclei may also cause large drops to grow by coalescing with small cloud droplets, resulting in enhanced convection (Braham Jr, 1974; Changnon et al., 1976; Johnson, 1982). There are many processes involved in urban rainfall modification and complex interactions among them. A meta-analysis by Liu and Niyogi (2019) concluded that although there is a general agreement that rainfall is modified in urban areas, there is a large variety of impacts reported in different studies (e.g., the type of effect, magnitude, and location).

There are observational findings indicating that the magnitude and frequency of heavy rainfall have increased in or around urbanized areas (e.g., Changnon & Westcott, 2002; Kishtawal et al., 2010; Lu et al., 2024; Niyogi et al., 2017; Shastri et al., 2015), however, there are not many studies that have assessed urban impacts on short-duration heavy rainfall events. These types of events often trigger urban pluvial floods, and their intensification is expected to increase urban flood risk further (Fowler, Ali, et al., 2021). So far, studies point towards an intensification of sub-daily rainfall extremes in urban areas compared to their surroundings (Huang et al., 2022; Li et al., 2020; P. Yang et al., 2017). Some observational studies have investigated urban impacts on heavy storms by analyzing high space-time resolution weather radar data (Kingfield et al., 2018; Lorenz et al., 2019; Niyogi et al., 2011; Yeung et al., 2015). However, there is no clear agreement among these studies regarding the urban impact on the properties of rainfall, such as on storms' extent and intensification, at the small-scale that was investigated (Lalonde et al., 2023). For example, in Indianapolis, US, downwind storm intensification and increased storm extent have been reported (Niyogi et al., 2011). Conversely, in Berlin, Germany, there are more cases of storm attenuation rather than intensification over and downwind of the city and reduced rain cell sizes (Lorenz et al., 2019).

Most of the urban rainfall literature has focused on studying urban influences on rainfall intensity and amount. Cities have been found to enhance rainfall mostly over and downwind of them (Liu & Niyogi, 2019), and sometimes upwind (Kingfield et al., 2018) or on their lateral sides (Dou et al., 2015; Y. Zhang et al., 2017). However, it is difficult to compare the findings among studies as different methodologies were used to assess the urban influence on rainfall intensification (Liu & Niyogi, 2019). As concluded by Lalonde et al. (2023), there is a current need to generalize these effects by conducting multi-city studies with consistent methodologies. Some studies have investigated the relationship between urban rainfall intensification and city characteristics (e.g., size, shape, population, urban heat, and aerosol emissions) (Ashley et al., 2012; Forney et al., 2022; Huff & Changnon, 1973; Kingfield et al., 2018; Lu et al., 2024; Schmid & Niyogi, 2013; Westcott, 1995; W. Zhang et al., 2022; Zhu et al., 2017). City size and population are the main characteristics that have shown a link to this intensification. These links have been mainly explored amongst US cities from usually the same region or through modeling experiments focused on one city. There is therefore a need to determine whether these relationships hold when comparing cities within different geographical regions, climates, and of largely different urban forms.

Aside from examining changes in rainfall intensity, it is also essential to examine how urban areas impact the spatial and temporal structure of rainfall; these two factors may be more important than rainfall intensification when it comes to triggering urban floods (Belachsen et al., 2017; Desa & Niemczynowicz, 1996; Peleg et al., 2022; Rozalis et al., 2010; Syed et al., 2003; L. Yang et al., 2016). For example, the findings of Zhou et al. (2021) indicate that more localized rainfall, but not necessarily more intense rainfall, can increase flood risk in urban areas. Storm spatial extent (i.e., area) and homogeneity (i.e., level of spatial variability of the rainfall intensities within a rain field) have been shown to vary with temperature in regional and global studies (Ghanghas et al., 2023; Lochbihler et al., 2017; Peleg et al., 2018; Wasko et al., 2016). Rainfall structure changes are

hypothesized to occur due to differences in dynamic and thermodynamic processes (Fowler, Lenderink, et al., 2021; Wasko et al., 2016). Because cities are generally warmer, drier, and rougher than their surroundings (Oke, 1973; Oke et al., 2017), it is expected that urban areas may alter storm structure as well. Some studies have found evidence of urban impacts on storm spatial structure by assessing changes in rain cell area or in storm splitting and merging in or around cities (Lorenz et al., 2019; Niyogi et al., 2011; L. Yang et al., 2014). Nevertheless, further research is needed to investigate how the spatial structure of rainfall is modified in different urban areas to determine if these patterns can be generalized to more cities.

Regarding the evolution and temporal structure of storms, several observational studies have shown that urban areas can also impact storms' life cycles. For example, urban areas have been found to experience more thunderstorm initiations compared to their surroundings, especially in the late afternoon (Changnon et al., 1976; Haberlie et al., 2015; Yeung et al., 2015), as well as increased rainfall frequency (Ashley et al., 2012; Burian & Shepherd, 2005; Changnon et al., 1976; Huff & Changnon, 1972; Kingfield et al., 2018; Marelle et al., 2020; Mote et al., 2007). There is also evidence that cities may contribute to the splitting and merging of storms upwind and downwind of them, respectively (Lorenz et al., 2019; Niyogi et al., 2011; L. Yang et al., 2014), or to increase storm attenuation over them (Lorenz et al., 2019). It is currently not possible to compare these effects and their magnitude amongst cities as most of these studies have been performed in single or few cities and the methodologies used to quantify these effects were different.

To improve the understanding of urban influences on extreme rainfall and enhance generalizability, we focus on evaluating various rainfall modification effects over eight different urban areas with diverse characteristics and climates, while utilizing the same methodology across all cities. We use high-resolution weather radar data to track the evolution of heavy rainfall and assess changes in its properties at minute and kilometer scales in urban areas and their surroundings. We aim to: (a) understand how different urban areas modify the intensity of convective rainfall events; (b) investigate how the rainfall spatial structure is altered due to the urban area; (c) evaluate changes in convective rainfall occurrence and storm life cycle; and (d) generalize our findings by exploring the links between these urban rainfall modification effects and city properties, such as city size, population, background climate, and type of urban form.

2. Methods and Data

2.1. Study Areas

We explored eight cities from different regions, characterized by diverse urban forms, background climates, and sizes (Figure 1 and Table 1). Four of the cities are located in Europe (Milan, Italy; Berlin, Germany; and London and Birmingham, United Kingdom), while the other four are located in the United States (Phoenix, Arizona; Charlotte, North Carolina; Atlanta, Georgia; and Indianapolis, Indiana). Besides the diversity in characteristics mentioned above, we chose these cities as they have available and good quality high-resolution weather radar data and are often exposed to heavy short-duration rainfall events in the summer months. Moreover, potential rainfall influences from other factors than the city are not foreseen as these cities are built on relatively flat terrain (i.e., minimal exposure to orographic effects), and they are not coastal or near large water bodies (i.e., rainfall is not potentially influenced by enhanced-lake humidity or breeze).

Although population density and/or impervious built-up area are usually used to classify urban areas (e.g., Kishtawal et al., 2010; Niyogi et al., 2017; Singh et al., 2016), there is no standardized method to define the boundaries and hence the size of urban areas (Kingfield et al., 2018). We used existing boundaries from regional agencies to define the extent of the urban areas. For the US cities, we used the 2020 US Census Bureau's urban area delineations, which use housing unit density and population criteria to define urban areas (Census Bureau, 2022). To obtain the urban boundaries of the remaining cities, we used local administrative unit boundaries from Eurostat (2020). We compared all urban area boundaries to maps of Local Climate Zones (LCZ) (Stewart & Oke, 2012) and if necessary (i.e., for London and Birmingham), we combined several of the units to obtain a larger boundary that was in better agreement with the LCZ maps (Figure 1).

2.2. Weather Radar Data Sets

Rainfall information is derived from weather radars, which are capable of providing continuous rainfall estimates in space and time (i.e., a time series of gridded rainfall fields) for the cities examined and their surrounding areas.

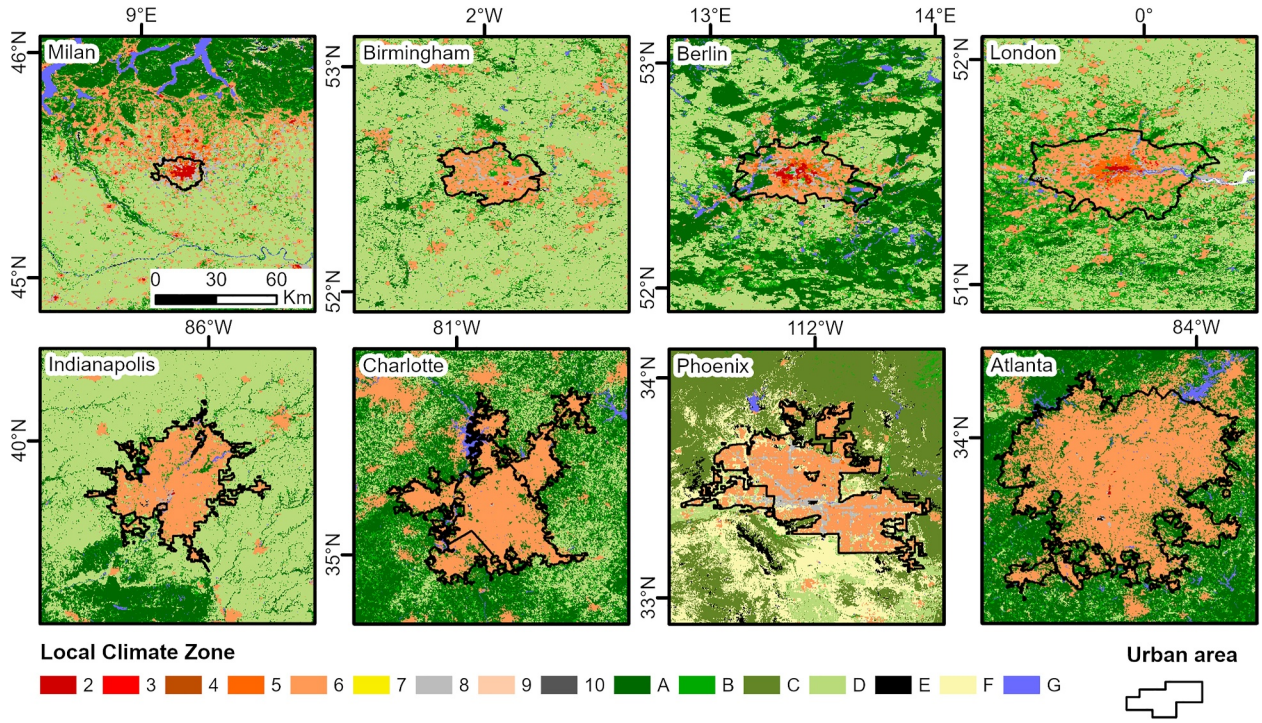

Figure 1. Maps of the study areas and their LCZs, using the same map scale. Urban boundaries are delineated in black. LCZ maps were obtained from Demuzere et al. (2019), Demuzere, Bechtel, et al. (2020), Demuzere, Hankey, et al. (2020), and Demuzere et al. (2021).

It should be noted that we have not used ground data from rain gauges, nor have we validated the rainfall data obtained from radars, but rather we have relied on quality control conducted by the data providers listed below. However, we do not expect this to have a significant impact on our analyses given that we are interested in relative, rather than absolute values. Given our interest in analyzing urban impacts on heavy short-duration rainfall, data were only obtained for the summer months (May to September/October), during which convective rainfall is more likely to occur (Barbero et al., 2019). Data span the period of 2015–2021 for all cities.

The European data sets are based on networks of C-band radars, with a 1 km and 5 min space–time resolution. Such small-scale resolution is necessary to examine urban-induced changes in rainfall that may trigger urban flash floods (Ochoa-Rodriguez et al., 2015) and C-band radars have been effectively used for this purpose in the past (Lorenz et al., 2019). We obtained radar data from the fourth-generation weather radar system of MeteoSwiss (Germann et al., 2015) for Milan, from the Radar Climatology (RADKLIM) data set (Winterrath et al., 2018)

Table 1
Characteristics of the Eight Studied Cities

Urban area	Lat. [°N]	Area [km^2]	Population [M]	Köppen classification
Milan	45.5	182	1.41	Cfa—Temperate, no dry season, hot summer
Birmingham	52.5	302	1.38	Cfb—Temperate, no dry season, warm summer
Berlin	52.5	892	3.66	Dfb—Cold, no dry season, warm summer
London	51.5	1,240	8.96	Cfb—Temperate, no dry season, warm summer
Indianapolis	39.8	1,870	1.70	Cfa—Temperate, no dry season, hot summer
Charlotte	35.2	2920	2.05	Cfa—Temperate, no dry season, hot summer
Phoenix	33.5	3,210	4.40	BWh—Arid, desert, hot
Atlanta	33.8	6,350	5.00	Cfa—Temperate, no dry season, hot summer

Note. Population data are for the year 2020 (sources: Census Bureau, 2022; DESTATIS, 2023; Istat, 2023; Nomis, 2020) and the Köppen-Geiger climate classification is from Beck et al. (2018).

10.1029/2024EF004505

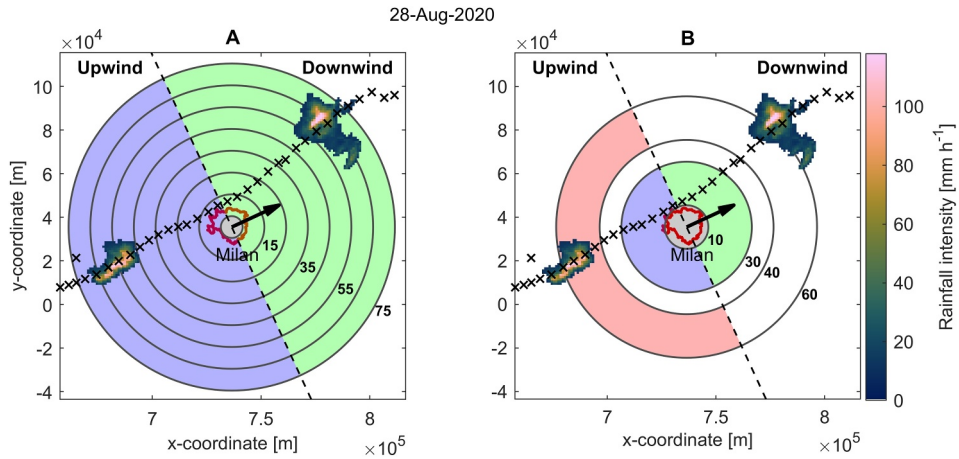

Figure 2. An example of a track's trajectory over Milan and how upwind and downwind distances are defined. The radar rain fields of two objects belonging to the track are displayed at two different times and the center of mass of each object pertaining to this track is marked with a cross. The mean direction of motion of the track is shown with a black arrow and the vector perpendicular to it defines the upwind and downwind areas, which are separated with a dashed line. Radial distances (in km) from the city center are labeled and depicted in gray lines. (a) 10-km wide bins are illustrated; upwind (downwind) bins are shaded in blue (green). (b) 20-km wide bins are illustrated; three urban bins and the upwind control bin shaded in red.

from the German Weather Service (DWD) for Berlin, and for the UK cities, we derived radar data from the Met Office's NIMROD product (Golding, 1998).

For the US cities, rainfall data were obtained from the Multi-Radar Multi-Sensor (MRMS) Surface Precipitation Rate product from the National Centers for Environmental Prediction (NCEP) (J. Zhang et al., 2016). As opposed to the European radar products, the MRMS data are based on networks of mainly S-band radars and are corrected with numerical weather prediction models. Nonetheless, similar to the C-band, it has been proven useful in capturing rainfall that causes flooding in urban areas (Gerard et al., 2021). MRMS has a space-time resolution of 1 km and 2 min; however, we used data every 4 min to closely match the resolution of the other products. We carefully examined the composite products for each of the cities, ensuring that each city has at least one radar coverage within a distance of acceptable operational range (up to 100 km) and that no radars were found within a distance of 6 km from the city center to eliminate the cone of silence effect. The radar data quality and some of its limitations are addressed in the Discussion section.

2.3. Urban Heat and Dry Island Data

To temporally cross-reference radar data patterns with diurnal UHI and urban dry island (UDI) patterns, we computed diurnal UHI and UDI cycles for the different urban areas. We used hourly air temperature and dew point temperature (TD) and/or relative humidity (RH) climate station data from at least one station near each city center and one from a rural surrounding area, for the whole study period (Table S1 in Supporting Information S1). We then standardized the UHI and UDI cycles by their maximum hourly value to be able to compare the diurnal patterns across cities.

2.4. Storm Tracking

We tracked the evolution of heavy rainfall in space and time using a storm-tracking algorithm developed by Moseley et al. (2019). Using similarity criteria, the algorithm identified a user-defined rainfall cluster (hereafter referred to as objects) in two consecutive time steps and derived the moving vector between them (Figure 2). We set the algorithm to identify connected grid points (objects) that contained rainfall intensity values over 10 mm hr^{-1} and that formed an area greater than 9 km^2. These imposed thresholds were chosen following Peleg and Morin (2012) to ensure that we track mostly the heavy-convective rain cells. Objects that overlapped between subsequent time steps were then linked into a track. The algorithm iteratively computed a mean advection velocity field after objects were identified to improve the identification of tracks when objects did not overlap due to being small and/or the advection velocity being high (Moseley et al., 2019).

We computed the mean direction of motion of each track and defined upwind and downwind locations for each track individually; objects with a center of mass before (after) the city center were classified as upwind (downwind). We considered objects from all tracks identified by the tracking algorithm that were less than 75 km away from the urban centers and that belonged to tracks with a lifetime greater than 15 min. We did not impose any further criteria to include or exclude tracks, hence tracks were included regardless of how close they moved from the urban centers or how their trajectories changed in space and time (i.e., whether and where they were initiated, terminated, bifurcated, split, or merged). An example of a storm-tracking procedure for a single track in the city of Milan is presented in Figure 2. The algorithm was also capable of identifying the "life cycle" of the tracked storms, namely where and when they initiated, terminated, split, or merged.

2.5. Evaluating Changes in Rain Cell Properties

We first determined how far upwind or downwind from the urban center each object was by calculating the radial distance from each object's weighted center of mass to the urban center. We then extracted different rain cell properties (mean intensity, maximum intensity, and area) for all objects from the tracks identified by the tracking algorithm. To assess the spatial structure of each rain field, we used a metric that quantifies grid-homogeneity, named Spatial Homogeneity (SH). This unitless metric was introduced by Ghanghas et al. (2023) and quantifies the spatial homogeneity of rain fields and can be used to compare rain fields of different intensities. To compute this metric for each object, we first centered each object's intensity field on a window of 17-by-17 grid cells using its weighted center of mass. This window size was chosen because it was large enough to generally cover object rainfall values over the 10 mm hr^{-1} threshold. Next, the intensity values of each radar grid cell were sorted in descending order and a cumulative normalization was performed, following Ghanghas et al. (2023):

$$\mathrm{SH} = \frac{\frac{1}{289} \times \sum_{i=0}^{288} P_i - \frac{P_0}{289}}{P_0 - \frac{P_0}{289}}, \tag{1}$$

where P_0 is the maximum and P_{288} the minimum intensity value of the window. This metric quantifies how much a particular rainfall field differs from a case where rainfall occurs only at the center pixel, relative to the difference between a case where there is only rainfall at the center and a case where all pixels have the same rainfall intensity value. More localized and convective rainfall fields will have a metric closer to zero, and more uniform and stratiform fields will have a metric closer to one. Figure 1 in Ghanghas et al. (2023) illustrates this concept.

Studies have shown that urban impacts on rainfall may occur at different locations within or near urban areas, and not only over or downwind of them (e.g., Changnon et al., 1976; Changnon & Westcott, 2002). For example, in some cases, reduced rainfall intensities and lightning activity have been observed directly over urban centers along with increased peaks in the city periphery (Lorenz et al., 2019; Shi et al., 2022), or on their lateral sides due to airflow bifurcation (Bornstein & Lin, 2000; Dou et al., 2015). Therefore, to explore where rainfall modification occurred within our study areas, we first explored changes in object properties (mean intensity, area, and SH) as a function of their distance from the city centers. We grouped all objects into 10-km wide bins and then compared the distributions of the different object properties between bins, up to 75 km upwind and downwind of the urban centers (Figure 2a). This relatively small bin size allowed us to detect changes at a fine spatial scale.

Next, to quantify changes in rainfall property from a surrounding control region to the urban area, we grouped objects into four larger bins (20-km wide). First, an upwind control bin (40–60 km from the city center) that served as a reference, and then, three urban bins: one positioned directly over the city center, and two bins adjacent to the latter (10–30 km upwind and downwind) (Figure 2b). The aim here was to obtain statistics of object properties over and near the edges of the urban areas as well as in a control region, at a coarser spatial scale and with increased sample size. We assume that the control bin is not influenced by the urban area and serves as a reference; this assumption is based on several studies indicating that urban impacts on rainfall upwind of cities are observed up to distances of approximately 30–40 km (Liu & Niyogi, 2019). We then calculated the maximum median change from the control to any of the three urban bins (as shown in Figure 2b). The statistical significance and confidence intervals of these median changes were evaluated using a non-parametric permutation test (Ernst, 2004). We then explored the relationship between the urban rainfall effects and city size, population, and average upwind storm intensity, by plotting these variables for all cities against each other.

2.6. Storm Evolution Patterns

We investigated urban impacts on the evolution of storms by comparing the frequency of different life cycle events (initiations, terminations, splits, and merges) between the control and urban bins (Figure 2b). We computed the total number of track initiations in each bin, and normalized each value by its bin's area, to account for the fact that bins further away from the city center had a larger area and therefore more rainfall occurrences. For the remaining track life cycle events, we normalized event occurrences by the total number of object occurrences in each bin. This was done to remove the effect introduced by changes in object occurrences (i.e., increased object occurrences results in increased amounts of other life cycle events). We then compared the frequency of all life cycle events between bins by performing a permutation test (Ernst, 2004). We also examined track initiation changes on an hourly basis since urban areas have been shown to increase rainfall occurrence, especially in the late afternoon hours (e.g., Ashley et al., 2012; Huff & Changnon, 1973; Westcott, 1995). Here, the same procedure was applied but data was binned into 5-hr wide rolling bins. The permutation test was also used to assess the differences in initiation frequency between the control and central urban bin at each 5-hr rolling bin.

3. Results

3.1. Changes in Rainfall Areal Mean Intensity

The distribution of the mean areal intensity of the objects is displayed in Figure 3. It illustrates increases in both means and medians near or over urban areas compared to upwind distances (40–70 km). Maximum increases were typically observed directly above the city centers, except for Birmingham and Berlin, which displayed lower intensities over the city but enhancements near their downwind and/or upwind edges (Figure 3 and Figure S1 in Supporting Information S1). The maximum median increases from the upwind regions (bins 35–75 km from the urban center) to the urban areas (extending 15 km from the urban centers) in Figure 3 were approximately 4% for

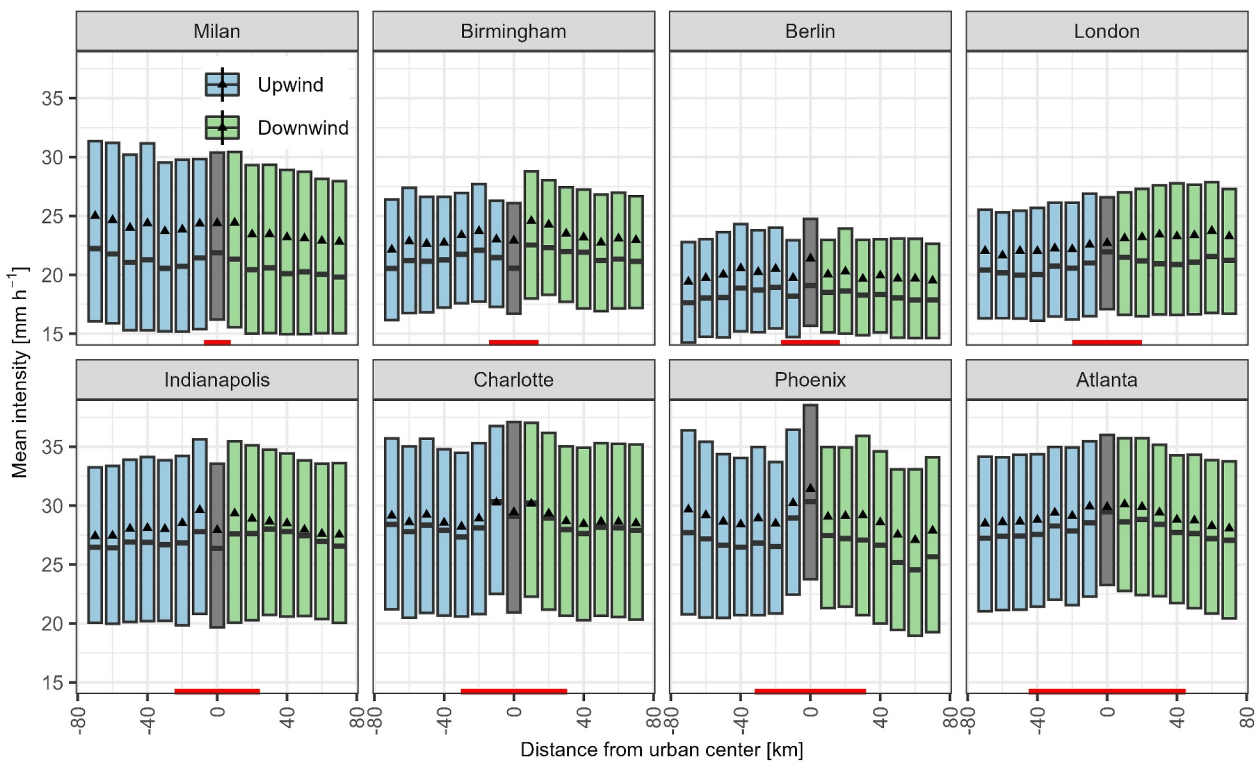

Figure 3. Box plots showing the distributions of object areal mean intensity at different distances from the urban centers. Upwind (downwind) distances are negative (positive) and are shaded in blue (green). The central line marks the median and the upper (lower) box borders, the 25th (75th) percentile. The mean of each distribution is marked with a black triangle. The extent of each city (average diameter) is marked with a red segment.

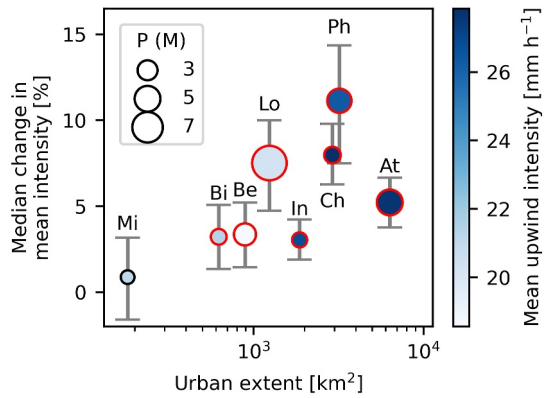

Figure 4. Maximum median increase in object areal mean intensity from the control to any of the three urban bins. The maximum median change is plotted against the size of the urban area. The color of the scatter points shows the average upwind storm intensity, its size represents the population (P), and a red outline indicates that the change in the median was statistically significant ($p < 0.05$). The error bars show the 5th–95th confidence intervals of the median differences.

Milan, 5% for Indianapolis, 8% for Atlanta and Berlin, 9% for Charlotte, 10% for Birmingham and London, and 15% for Phoenix.

We then quantified the maximum control-to-urban changes in mean object intensity using larger bins (Figure 4). The median control-to-urban changes were statistically significant across all cities, except for Milan (Figure 4). We found that larger cities tended to show greater intensification effects. For example, in the three smallest cities (i.e., areas smaller than 1,000 km^2), mean rainfall intensified by 0.9%–3.4%. In contrast, the three largest cities (i.e., with areas above 2000 km^2) showed an intensification of 5.2%–11%. Cities with generally higher mean storm intensities showed greater rainfall intensification effects as well; however, it is noteworthy that these cities were also the largest. The intensification appeared to be less related to population than to city size. Figure S1 in Supporting Information S1 displays control-to-urban changes in mean object intensity at all three urban bins. As also evident in Figure 3, there are differences in the magnitude and direction of the rainfall effect across the different urban bins, however, the positive correlation between city extent and rainfall intensification is still apparent.

3.2. Diurnal Intensification Patterns

We next explored hourly control-to-urban rainfall intensity changes downwind, upwind, and over the cities (Figure 5) and found that the magnitude of the intensification generally varied for different times of the day. Much higher intensification rates were displayed when examining rainfall intensification on an hour-by-hour basis, compared to Figure 4, where the effects are averaged over the whole day. In addition, some urban areas only displayed significant changes at specific times

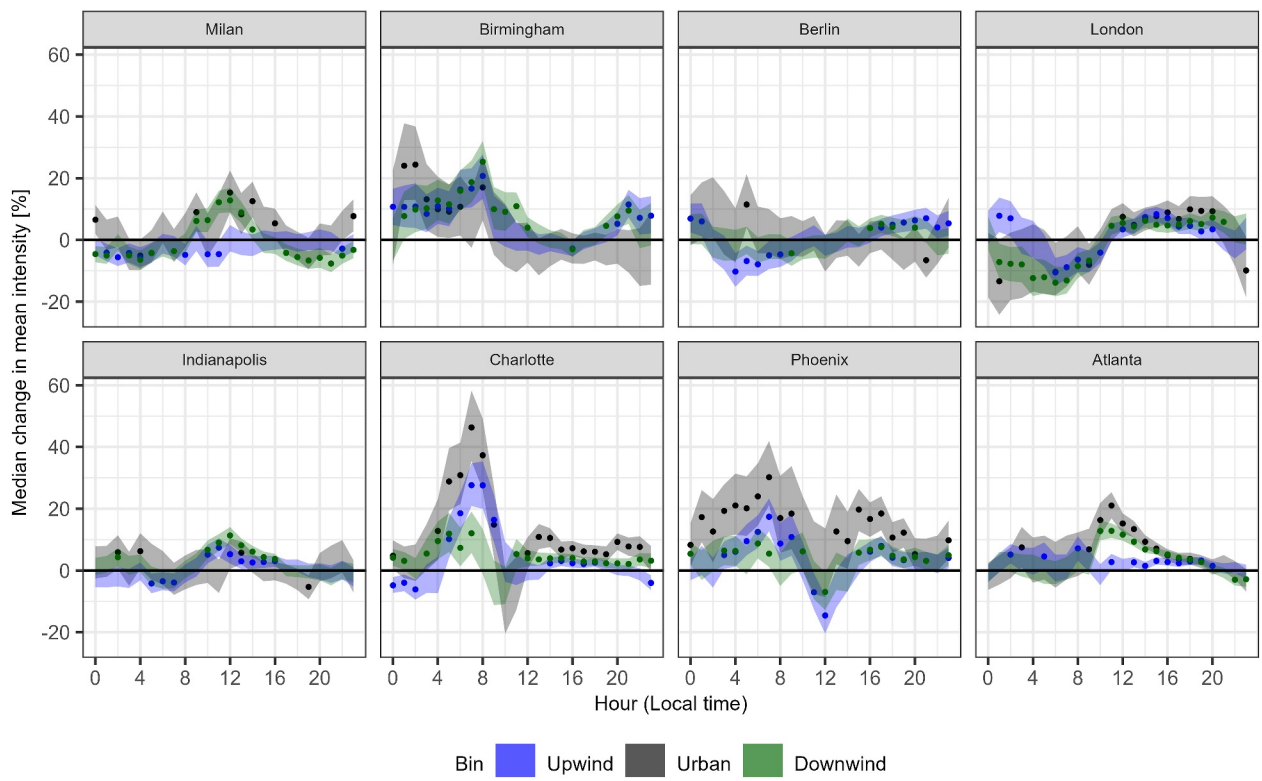

Figure 5. Diurnal cycles of median changes in object mean intensity, from the control to the urban bins. The median differences were computed over moving windows of 5 hours. The shaded areas show the 5th–95th confidence intervals of the median differences. The dots indicate that the median changes at a particular time bin were significant ($p < 0.05$).

10.1029/2024EF004505

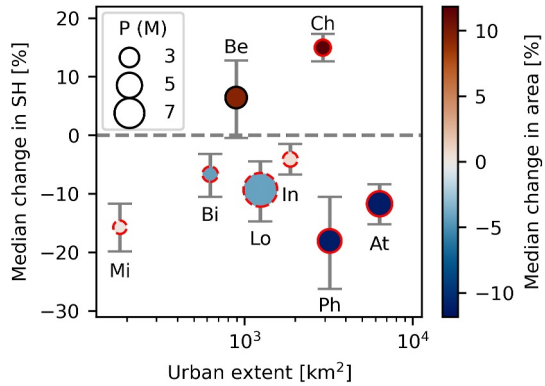

Figure 6. Maximum median change in object spatial heterogeneity (SH index) from the control to any of the three urban bins, plotted against city size. An increase (decrease) in SH represents a decrease (increase) in rainfall heterogeneity. The color of the scatter points shows the median rural-to-urban change in object area and its size represents the population (P). A red outline indicates that the change in median object SH was statistically significant ($p < 0.05$). A solid (dashed) outline indicates that the change in median object area was (not) statistically significant.

and in some cases, opposite effects were observed during different periods. For example, in Milan, significant intensification only occurred around the afternoon hours, ranging from 5% to 15%. Birmingham displayed intensification effects only during the nighttime hours, between 5% and 11%, upwind, over, and downwind of the city. Atlanta experienced most of the intensification during the daytime hours, from 3% to 21%, both over the city and downwind. Both Charlotte and Phoenix showed significant intensification during most times of the day, mostly over the cities but also upwind and downwind. Over these cities, rainfall intensification ranged from 2% to 46% and 8%–30%. Berlin and London both showed opposite effects at different times of the day. In Berlin, rainfall intensified in the upwind and downwind regions, from 4% to 7%, in the late afternoon until midnight, and in the early morning hours, upwind rainfall was weakened between 5% and 10%. In London, rainfall intensified from the afternoon until nighttime, between 5% and 10%, and weakened in the upwind and downwind regions during the night, by 7%–14%.

3.3. Changes in Rainfall Spatial Structure

Control-to-urban changes in the spatial structure of objects (SH index and area) are shown in Figure 6 and Figures S2, and S3 in Supporting Information S1. All urban areas, except Berlin, showed statistically significant changes in object SH in at least one of the urban bins (Figures 6 and Figure S1 in Supporting Information S1). Changes in object area were significant over three cities. Phoenix and Atlanta showed significant changes in both SH and area; SH medians decreased by 18% and 12%, respectively, over the urban areas, compared to the control region (Figure 6). Median object area decreased by 11% in both cases. In Milan, Birmingham, London and Indianapolis, median object SH decreased between 4% and 16%, however, the changes in area were not statistically significant. Overall, most urban areas displayed an increase in rainfall heterogeneity and a decrease or no change in the object area. The opposite occurred in two cities (Berlin and Charlotte), which showed increased rainfall homogeneity by 6% and 15%, and increased object area at the order of 9% and 12%. We found no evidence of links between urban impacts on rainfall spatial structure and city characteristics, such as urban extent and population size.

3.4. Storm Life Cycles

Six out of the eight urban areas experienced more track initiations compared to their control regions. These differences were statistically significant in five cities: Milan, London, Indianapolis, Charlotte, and Atlanta (Figure S4 in Supporting Information S1). These cities showed increases of 18%–42%, and the maximum increase usually occurred directly over them. The diurnal patterns of initiations for the control and urban bins are presented in Figure 7, and their difference is in Figure 8. Both the control and urban bins displayed diurnal patterns, with minimum occurrences at night and maximum values in the late afternoon (Figure 7). Similar to Figure 5, we observed variations in the differences between control and urban bins at different times of the day, compared to the average over the entire day (Figure 8 vs. Figure S4 in Supporting Information S1). Most statistically significant control-to-urban differences occurred between the afternoon and late evening hours in London and Atlanta, which showed maximum increases of approximately 85%. In Birmingham, Indianapolis, and Charlotte, the highest increases (from 42% to 126%) occurred between the late afternoon and evening hours. In Milan, the largest increases (up to 54%) happened at night. Berlin and Phoenix did not display statistically significant changes in track initiation patterns. Unlike for storm initiation patterns, there were no significant changes in the number of track termination, splitting, and merging events between the control and urban regions, except for increased storm splitting in Berlin (Figure S4 in Supporting Information S1).

Next, we compared initiation patterns with diurnal UHI and UDI cycles. UHI diurnal cycles showed similar patterns as the UDI, when computed with RH data. When computing the UDI with TD data, we found the largest urban moisture deficits earlier in the day (usually in the afternoon to evening hours, instead of at nighttime). Figure 7 and Figure S5 in Supporting Information S1 show that peak control-to-urban initiation differences did not generally occur during peak UHI hours or when rural-to-urban RH differences were highest. This only happened in Milan and Birmingham, where both peaked at night or in the evening, respectively. In Atlanta,

10.1029/2024EF004505

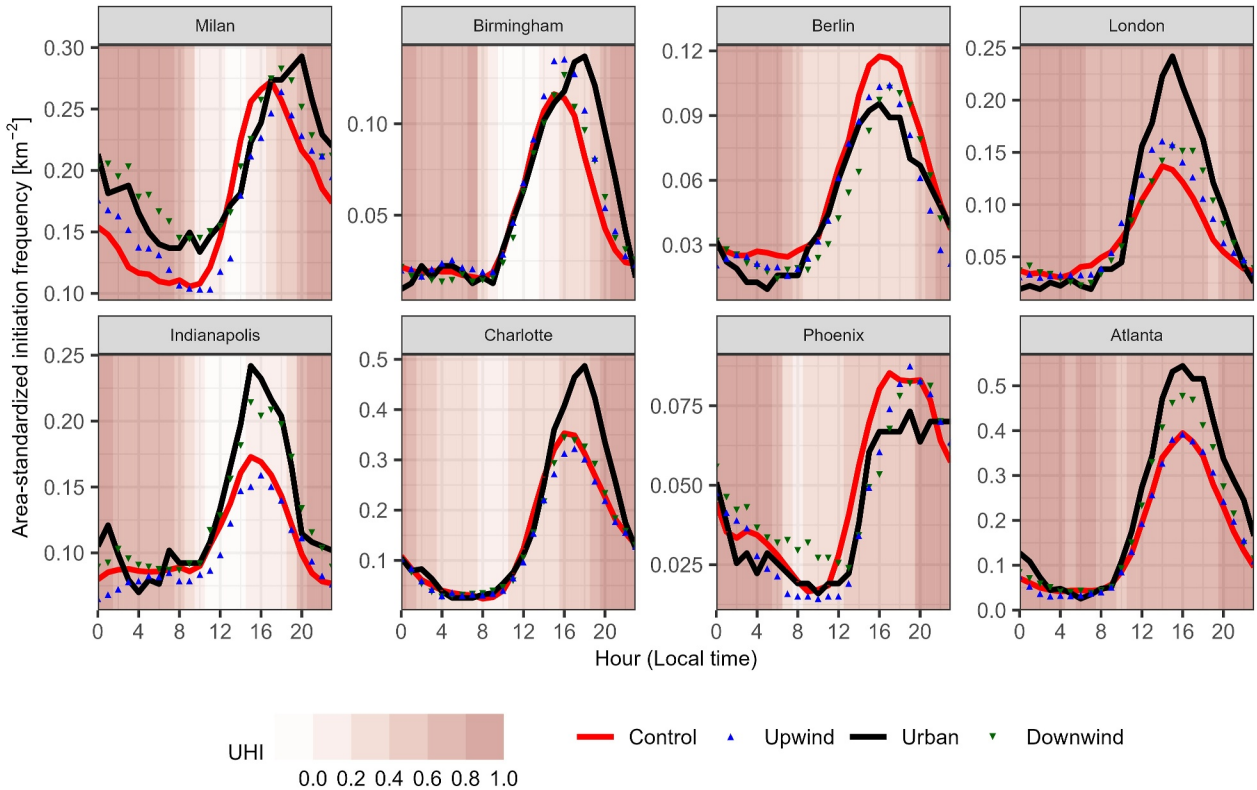

Figure 7. Diurnal cycles of track initiation frequency in the control and urban bins. A moving mean calculation was applied to the data using a rolling window width of 5 hr. The occurrences in each bin were normalized by the area of each bin. The background fill color represents the hourly mean standardized UHI values.

Charlotte and Indianapolis, the highest track initiation differences were found when rural-to-urban TD differences were largest (i.e., when the moisture deficit was largest). Or, in the case of London, when the urban moisture island was at its minimum (Figure S6 in Supporting Information S1).

4. Discussion and Implications

Our results have shown that heavy rainfall is intensified directly over cities or in two cases, over the city boundaries. As discussed in Liu and Niyogi (2019), downwind rainfall enhancement seems to be a commonly highlighted result in the literature, however, over-the-city effects seem to occur as well, and with a similar magnitude. Differences in the reported location of the urban effect (upwind, over, downwind, or laterally) appear to be linked to study methodologies (e.g., observational vs. modeling studies, and case study vs. climatological studies) (Liu & Niyogi, 2019). It is thus difficult to compare the location of the urban effect across studies in different cities and based on different methodologies. Here, we have found that urban rainfall effects may occur at different locations relative to the city centers, depending on the city (Figure 3). Drivers for these differences could include the climatology of the area, orographic forcing in the surroundings, the presence of aerosols, or large gradients in temperature and humidity at the urban boundaries due to the land-surface discontinuity.

We next explored intensification links to different city characteristics, such as population, urban form, and mean storm intensity, and found that intensification is positively related to city size (Figure 4). These results are in agreement with Schmid and Niyogi (2013) and Forney et al. (2022), who showed that urban rainfall modification increased linearly with city size. Since demographic projections show that urban population will globally increase in the future (UN-DESA, 2018) and this is expected to result in urban land expansion (Seto et al., 2010), our results point toward increased intensification of (convective) summer rainfall that may lead to increase in future flood risk in large cities. A factor that was not explored in our study but that may be linked to the rainfall modification potential may be city shape. As discussed by W. Zhang et al. (2022), different city shapes may result in different urban-rural circulation patterns and result in different rainfall anomalies. Future studies should further

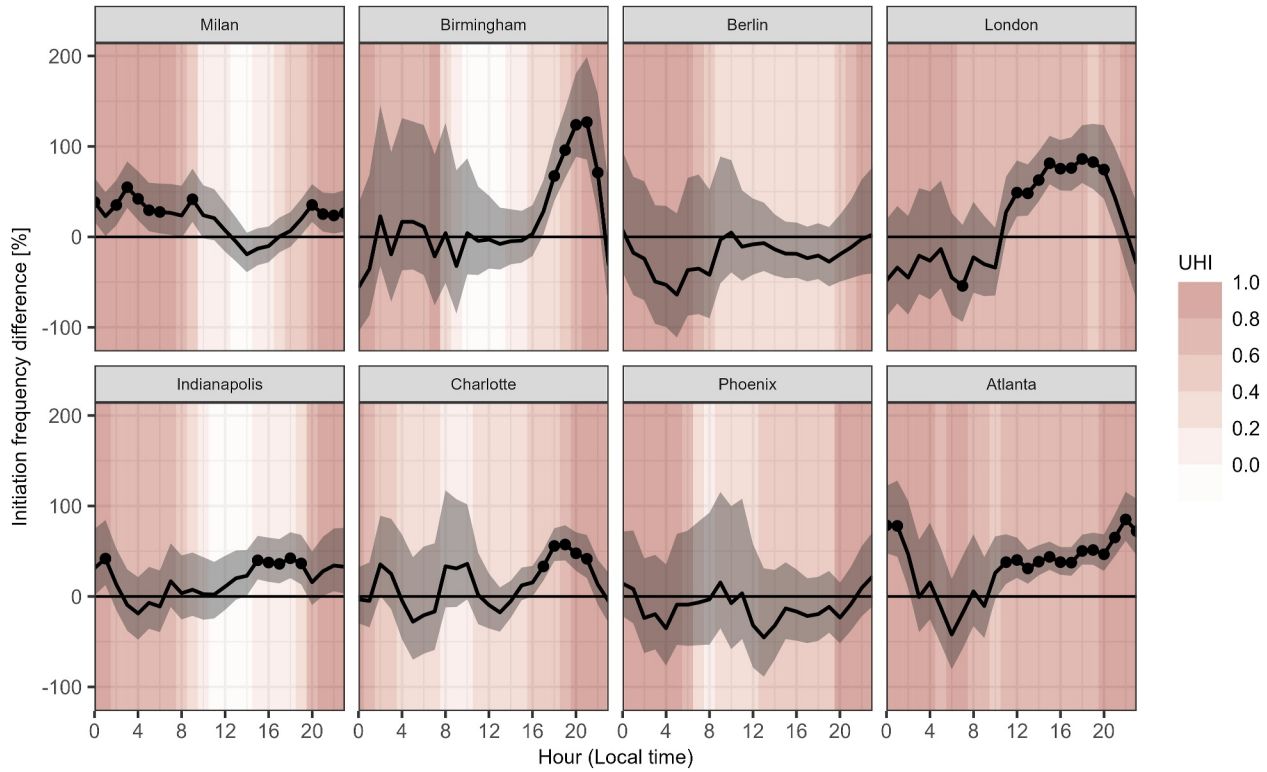

Figure 8. Diurnal cycles of track initiation frequency difference between the control and central urban bin. A moving mean calculation was applied to the data using a rolling window width of 5 hr. The shaded area shows the 5th–95th confidence interval of the differences. The dots indicate that the differences at a particular time bin were significant ($p < 0.05$). The background fill color represents the hourly mean standardized UHI values.

investigate links between rainfall modification and city properties (especially size and shape) by investigating additional urban areas from different regions and local climates, with consistent methodologies. It is important to note that the reported city sizes are determined by the urban delineation method used. Defining urban boundaries with demographic and land cover data has potential limitations, because urban influence may extend beyond landform changes (Niyogi et al., 2017; Singh et al., 2020). As suggested by Singh et al. (2020), several comprehensive approaches can be used to define urban areas, which can be applied in future research.

We observed distinct diurnal patterns of rainfall intensification across the different cities (Figure 5), with intensification occurring both during the daytime and/or nighttime hours, depending on the city. The former may occur because the UHI circulation is expected to be stronger at daytime compared to nighttime (even though the UHI tends to be lower) because increased surface heating results in enhanced vertical mixing (Niyogi et al., 2011). Additionally, we note that a drier urban near-surface environment (i.e., apparent in most of the studied cities; Figure S6 in Supporting Information S1) may increase atmospheric instability and result in moisture convergence over the city (Argüeso et al., 2016; Li et al., 2020). Yet, nighttime UHI peaks have also been reported to cause rainfall enhancement over or downwind of inland cities due to increased urban instability (Ganeshan et al., 2013; Lorenz et al., 2019). To understand why different diurnal patterns of rainfall modification are being observed in different cities, these patterns should be investigated across more cities, and the driving processes should be explored through modeling studies.

The accuracy of the urban rainfall intensification quantification was in some cases limited by the radar data quality, and resulted in under- and over-estimations in some study areas. The radar data quality was checked by exploring potential beam blockages and ground echoes that may systematically bias the estimates in specific locations. Maps of mean object rainfall intensity and total rainfall occurrence revealed some issues in a few cities. For example, the weather radar in Indianapolis was located close to the city center (approximately 12 km southwest of it) and this resulted in an area of underestimated rainfall intensities and reduced rainfall occurrence. In this case, we expect that the rainfall intensification effect over the city is higher than what is observed in

Figures 3 and 4. Charlotte and Phoenix presented partial beam blockages within or around the city areas, potentially resulting in an overestimated rainfall intensification effect. Although we found some areas within the study domains with decreased radar quality, we expect that the impacts on the results are decreased due to the Lagrangian approach adopted.

To compare urban impacts across the different studied cities in a consistent manner, we binned data and compared it across bins of the same size for all cities. This framework may be limiting when the studied cities have a wide range of sizes. For example, in the case of Atlanta, the largest city studied, urban rainfall intensification might be underestimated since the control bin is close to the city boundaries and may already be experiencing some urban influences. In the case of Milan, the control bin did contain orographic influences, due to the presence of the Alps, starting approximately 40 km north of the city center. This resulted in intensification underestimation since intensities over the mountainous regions were higher than in the adjacent flat terrain. There are alternative ways of defining the rural (or in our case, the control) and urban influenced regions, as for example, Niyogi et al. (2011) used a threshold that was twice the city size. Future studies could consider using a "moving threshold," where the control bin is shifted further upwind if a city is larger or closer to the city if smaller.

Aside from increased urban rainfall intensities, we also detected changes in rainfall spatial structure over urban areas (Figure 6). Rainfall spatial structure changes with temperature have been shown to vary regionally (e.g., Ghanghas et al., 2023; Lochbihler et al., 2017; Peleg et al., 2018; Wasko et al., 2016). Our results agree with the expected regional changes in the spatial extent of short-duration extreme precipitation due to temperature increases, as reported by Ghanghas et al. (2023). In most cities, a decrease in spatial homogeneity was observed compared to the surrounding areas. This suggests that rainfall is more localized and clustered over the cities and that there is a re-distribution of moisture from the low to the high intensities. This implies that in most of the studied cities, urban flood risk may increase, given that rainfall extremes are more spatially concentrated and also more intense. L. Yang et al. (2015) discussed the potential for underestimating flood magnitudes if spatial rainfall patterns are not taken into account.

Over the cities of Berlin and Charlotte, we found increases in rainfall homogeneity (i.e., rainfall becomes less spatially clustered); the results in Berlin are also in agreement with Ghanghas et al. (2023), who reported an increase in spatial homogeneity with increased temperatures in central Europe. However, the results in Charlotte do not follow the expected spatial rainfall modifications due to background temperature increase. Further studies are needed to understand the dynamic and thermodynamic mechanisms behind these spatial structure changes and the differences across cities. The observed spatial structure changes are likely not only due to rural-to-urban temperature changes but also to other urban effects, such as moisture, aerosols and increased surface roughness (Han et al., 2014). This may also explain why we have observed larger changes in SH over urban areas, compared to the anticipated change in SH magnitude with temperature reported by Ghanghas et al. (2023), when considering the average UHI magnitude. Additionally, the changes we have observed in rainfall spatial structure are most probably sensitive to the rainfall intensity threshold used (10 mm hr^{-1}).

Assessing changes in storm life cycle over the urban areas revealed significant increases in convective rainfall initiation over six cities, at least at some time of day (Figure 8). Peak initiation differences between rural and urban areas occurred in the late afternoon to evening hours, and not usually during peak UHI hours. This is generally the time when the urban boundary layer (UBL) is most unstable (Lemonsu & Masson, 2002; Rotach et al., 2005). This indicates that, generally, boundary layer instability is preferable for the initiation of new convective cells and that high rural-to-urban temperature differences together with a more stable UBL (e.g., during nighttime hours) are not sufficient to trigger convective initiations. Furthermore, we found that in some cities, these peaks occurred when rural-to-urban moisture deficits were the highest (Figure S6 in Supporting Information S1). The warmer and drier urban environment creates favorable conditions for convection, that is, the thermodynamic gradient results in increased vertical uplift and moisture convergence, where moist air is brought from the surrounding areas and lifted over the city (Argüeso et al., 2016; Li et al., 2020). Our results are in agreement with Westcott (1995), who found maximum increases in lightning flash frequency (a proxy for convective activity) at this time of day in the Midwestern US, and with Burian and Shepherd (2005), who found greater rainfall amounts and occurrences between noon and midnight over Houston, US, compared to its surroundings. Two of the studied cities, Phoenix and Berlin, did not show increases in storm initiations over them. In Phoenix, this may be a result of orographic effects; we found an area of increased rainfall occurrence over the mountains northeast of the city, therefore increasing initiation occurrences in the control region. In Berlin, this

might be due to lower radar quality, since the control bin was sometimes placed over an area where the coverage of two radar systems intersected, which displayed anomalously high rainfall occurrences.

A few studies have reported increases in storm splitting and merging in or around cities (Lorenz et al., 2019; Niyogi et al., 2011; L. Yang et al., 2014). While we did observe an increase in the frequency of splitting and/or merging in some urban regions relative to the increases in rainfall occurrence, these changes were not statistically significant. Berlin was the only city that displayed significant increases in storm splitting over it (Figure S4 in Supporting Information S1). We therefore did not find sufficient evidence to support that, in general, urban areas changed patterns of storm splitting, merging, or terminating. These effects might only take place in some cities and not in others, for example, Yeung et al. (2015) also investigated storm splitting over New York City, US, and found no urban impacts on storm splitting. However, our results may be sensitive to the ability of the storm tracking algorithm to correctly identify these events.

Prior to this work, several city-based studies have conducted detailed weather radar data analysis on the impacts of urban areas on rainfall. Our results are in general agreement with the results reported. For example, Lorenz et al. (2019) generally reported the following in Berlin: rainfall intensification at the city periphery exclusively (usually upwind), over-the-city attenuation during the daytime or nighttime intensification over the city, and potential increased storm splitting over the city. We found significant rainfall intensification only in the city peripheries (i.e., the upwind and downwind urban bins, Figure S1 in Supporting Information S1) in the evening to early night hours (Figure 5), upwind rainfall attenuation in the early morning hours (Figure 5), and significant increases in storm splitting over the city (Figure S4 in Supporting Information S1). In Indianapolis, Niyogi et al. (2011) observed significantly more rain cells in the downwind than upwind regions and suggested this may be due to increased rain cell splitting or increased initiations. Here, we found increased rainfall occurrence in the late afternoon hours over and downwind of the city, which was explained by the latter (Figures 7 and 8). They also found a greater number of smaller cells in the downwind region and larger cells upwind. Although we did not observe this, we instead found considerable increases in rain cell size over the city (Figures S1 and S3 in Supporting Information S1). In Atlanta, Mote et al. (2007) pointed to rainfall enhancements mainly over the urban core and downwind (eastern) part of the city. Our results also displayed maximum intensification in those locations (Figure S1 in Supporting Information S1 and Figure 3). They also reported the highest downwind rainfall rates in the evening to midnight hours, and although we did not spot maximum intensification then (we found it occurred around midday; Figure 5), we found that these hours showed the highest initiation occurrences (Figure 8). The general agreement of our results with these detailed city-specific analyzes reveals that our methodology can capture urban impacts across different study areas.

5. Conclusions

We have presented a climatological analysis of the space-time property changes of intense summertime (convective) rainfall in urban areas. Using high-resolution weather radar data, we examined eight urban areas located in different geographical regions and with varying climates. Heavy summertime storms were tracked with a storm-tracking algorithm, allowing us to detect where urban impacts occurred, relative to each storm's direction of motion. Our results suggest that cities and their surroundings act to critically modify rainfall properties. Rainfall intensities are higher over cities and/or their peripheries, compared to their surroundings and this effect is positively linked to the city size (i.e., the larger the metropolitan area, the more intense the rainfall is). The spatial structure of rainfall is altered over cities, and in most cases, rainfall becomes more heterogeneous—that is more localized and spatially clustered. Lastly, urban areas experience more initiations of heavy rainfall, especially in the afternoon to evening hours. Our findings suggest that further urbanization, which would result in larger and denser cities, has the potential to substantially enhance changes in the properties of heavy summer rainfall. As a result of these changes, the flood risk in large cities may be exacerbated beyond what is expected due to climate change-induced rainfall intensification and the increase in impervious surfaces.

Data Availability Statement

We used the following weather radar data sets for our analyzes: the fourth-generation weather radar system of MeteoSwiss (Germann et al., 2015); the RADKLIM quasi gauge-adjusted five-minute precipitation rate from the Deutscher Wetterdienst (DWD) (Winterrath et al., 2018); the 1 km Resolution UK Composite Rainfall Data from

the Met Office Nimrod System (Golding, 1998) via the NCAS British Atmospheric Data Centre (Met Office, 2003); and the Multi-RADAR Multi-Sensor (MRMS) Archiving (J. Zhang et al., 2016) via the Iowa Environmental Mesonet (NOAA, 2023a). We obtained the following urban boundary data sets: the administrative boundary data sets for European study areas for 2020 from Eurostat (2020); 2020 Berlin population data from DESTATIS (2023); 2020 Milan population data from Istat (2023); 2020 London and Birmingham population data from Nomis (2020); and the 2020 US urban area delineations and population data from the Census Bureau (2022).

Acknowledgments
This study was supported by the Swiss National Science Foundation (SNSF), Grant 194649 ("Rainfall and floods in future cities"). We thank the two reviewers for their constructive feedback and significant contributions, which have helped to improve the quality of the manuscript. The scientific color map in Figure 2 is from Crameri (2018).

References

Argüeso, D., Di Luca, A., & Evans, J. P. (2016). Precipitation over urban areas in the western maritime continent using a convection-permitting model. *Climate Dynamics*, *47*(3), 1143–1159. https://doi.org/10.1007/s00382-015-2893-6

Ashley, W. S., Bentley, M. L., & Stallins, J. A. (2012). Urban-induced thunderstorm modification in the southeast United States. *Climatic Change*, *113*(2), 481–498. https://doi.org/10.1007/s10584-011-0324-1

Barbero, R., Fowler, H. J., Blenkinsop, S., Westra, S., Moron, V., Lewis, E., et al. (2019). A synthesis of hourly and daily precipitation extremes in different climatic regions. *Weather and Climate Extremes*, *26*, 100219. https://doi.org/10.1016/j.wace.2019.100219

Beck, H. E., Zimmermann, N. E., McVicar, T. R., Vergopolan, N., Berg, A., & Wood, E. F. (2018). Present and future köppen-geiger climate classification maps at 1-km resolution. *Scientific Data*, *5*(1), 180214. https://doi.org/10.1038/sdata.2018.214

Belachsen, I., Marra, F., Peleg, N., & Morin, E. (2017). Convective rainfall in a dry climate: Relations with synoptic systems and flash-flood generation in the dead sea region. *Hydrology and Earth System Sciences*, *21*(10), 5165–5180. https://doi.org/10.5194/hess-21-5165-2017

Bornstein, R., & Lin, Q. (2000). Urban heat islands and summertime convective thunderstorms in Atlanta: Three case studies. *Atmospheric Environment*, *34*(3), 507–516. https://doi.org/10.1016/S1352-2310(99)00374-X

Braham Jr, R. R. (1974). Cloud physics of urban weather modification—A preliminary report. *Bulletin of the American Meteorological Society*, 100–106.

Burian, S. J., & Shepherd, J. M. (2005). Effect of urbanization on the diurnal rainfall pattern in Houston. *Hydrological Processes*, *19*(5), 1089–1103. https://doi.org/10.1002/hyp.5647

Census Bureau. (2022). 2020 Census qualifying urban areas and final criteria clarifications [Dataset]. https://www.federalregister.gov/documents/2022/12/29/2022-28286/2020-census-qualifying-urban-areas-and-final-criteria-clarifications

Changnon, S. A., Semonin, R. G., & Huff, A. (1976). A hypothesis for urban rainfall anomalies. *Journal of Applied Meteorology*, *15*(6), 544–560. https://doi.org/10.1175/1520-0450(1976)015<0544:ahfura>2.0.co;2

Changnon, S. A., & Westcott, N. E. (2002). Heavy rainstorms in Chicago: Increasing frequency, altered impacts, and future implications 1. *Journal of the American Water Resources Association*, *38*(5), 1467–1475. https://doi.org/10.1111/j.1752-1688.2002.tb04359.x

Crameri, F. (2018). Geodynamic diagnostics, scientific visualisation and staglab 3.0. *Geoscientific Model Development*, *11*(6), 2541–2562. https://doi.org/10.5194/gmd-11-2541-2018

Demuzere, M., Bechtel, B., Middel, A., & Mills, G. (2019). Mapping Europe into local climate zones. *Public Library of Science ONE*, *14*(4), e0214474. https://doi.org/10.1371/journal.pone.0214474

Demuzere, M., Bechtel, B., Middel, A., & Mills, G. (2020). European lcz map [Dataset]. *Figshare*. https://doi.org/10.6084/m9.figshare.13322450.v1

Demuzere, M., Hankey, S., Mills, G., Zhang, W., Lu, T., & Bechtel, B. (2020). Combining expert and crowd-sourced training data to map urban form and functions for the continental us. *Scientific Data*, *7*(1), 264. https://doi.org/10.1038/s41597-020-00605-z

Demuzere, M., Hankey, S., Mills, G., Zhang, W., Lu, T., & Bechtel, B. (2021). Conus-wide lcz map and training areas [Dataset]. *Figshare*. https://doi.org/10.6084/m9.figshare.11416950.v2

Desa, M. M. N., & Niemczynowicz, J. (1996). Spatial variability of rainfall in Kuala Lumpur, Malaysia: Long and short term characteristics. *Hydrological Sciences Journal*, *41*(3), 345–362. https://doi.org/10.1080/02626669609491507

DESTATIS. (2023). Population: Administrative districts, reference date [Dataset]. https://www-genesis.destatis.de/genesis//online?operation=table&code=12411-0015&bypass=true&levelindex=0&levelid=1694425319807

Dou, J., Wang, Y., Bornstein, R., & Miao, S. (2015). Observed spatial characteristics of Beijing urban climate impacts on summer thunderstorms. *Journal of Applied Meteorology and Climatology*, *54*(1), 94–105. https://doi.org/10.1175/JAMC-D-13-0355.1

Ernst, M. D. (2004). Permutation methods: A basis for exact inference. *Statistical Science*, *19*(4), 676–685. https://doi.org/10.1214/088342304000000396

Eurostat. (2020). Urban audit 2020 - Area management [Dataset]. https://gisco-services.ec.europa.eu/distribution/v2/urau/

Forney, R. K., Debbage, N., Miller, P., & Uzquiano, J. (2022). Urban effects on weakly forced thunderstorms observed in the Southeast United States. *Urban Climate*, *43*, 101161. https://doi.org/10.1016/j.uclim.2022.101161

Fowler, H. J., Ali, H., Allan, R. P., Ban, N., Barbero, R., Berg, P., et al. (2021). Towards advancing scientific knowledge of climate change impacts on short-duration rainfall extremes. *Philosophical Transactions of the Royal Society A: Mathematical, Physical & Engineering Sciences*, *379*(2195), 20190542. https://doi.org/10.1098/rsta.2019.0542

Fowler, H. J., Lenderink, G., Prein, A. F., Westra, S., Allan, R. P., Ban, N., et al. (2021). Anthropogenic intensification of short-duration rainfall extremes. *Nature Reviews Earth & Environment*, *2*(2), 107–122. https://doi.org/10.1038/s43017-020-00128-6

Ganeshan, M., Murtugudde, R., & Imhoff, M. L. (2013). A multi-city analysis of the UHI-Influence on warm season rainfall. *Urban Climate*, *6*, 1–23. https://doi.org/10.1016/j.uclim.2013.09.004

Gerard, A., Martinaitis, S. M., Gourley, J. J., Howard, K. W., & Zhang, J. (2021). An overview of the performance and operational applications of the MRMS and flash systems in recent significant urban flash flood events. *Bulletin of the American Meteorological Society*, *102*(11), E2165–E2176. https://doi.org/10.1175/BAMS-D-19-0273.1

Germann, U., Boscacci, M., Gabella, M., & Sartori, M. (2015). Peak performance: Radar design for prediction in the Swiss Alps. *Meteorological Technology International*, 42–45.

Ghanghas, A., Sharma, A., Dey, S., & Merwade, V. (2023). How is spatial homogeneity in precipitation extremes changing globally? *Geophysical Research Letters*, *50*(16), e2023GL103233. https://doi.org/10.1029/2023GL103233

Golding, B. W. (1998). Nimrod: A system for generating automated very short range forecasts. *Meteorological Applications*, *5*(1), 1–16. https://doi.org/10.1017/S1350482798000577

Haberlie, A. M., Ashley, W. S., & Pingel, T. J. (2015). The effect of urbanisation on the climatology of thunderstorm initiation. *Quarterly Journal of the Royal Meteorological Society*, *141*(688), 663–675. https://doi.org/10.1002/qj.2499

Han, J.-Y., & Baik, J.-J. (2008). A theoretical and numerical study of urban heat island–induced circulation and convection. *Journal of the Atmospheric Sciences*, *65*(6), 1859–1877. https://doi.org/10.1175/2007JAS2326.1

Han, J.-Y., Baik, J.-J., & Lee, H. (2014). Urban impacts on precipitation. *Asia-Pacific Journal of Atmospheric Sciences*, *50*(1), 17–30. https://doi.org/10.1007/s13143-014-0016-7

Haywood, J., & Boucher, O. (2000). Estimates of the direct and indirect radiative forcing due to tropospheric aerosols: A review. *Reviews of Geophysics*, *38*(4), 513–543. https://doi.org/10.1029/1999RG000078

Huang, J., Fatichi, S., Mascaro, G., Manoli, G., & Peleg, N. (2022). Intensification of sub-daily rainfall extremes in a low-rise urban area. *Urban Climate*, *42*, 101124. https://doi.org/10.1016/j.uclim.2022.101124

Huff, F. A., & Changnon, S. A. (1972). Climatological assessment of urban effects on precipitation at St. Louis. *Journal of Applied Meteorology and Climatology*, *11*(5), 823–842. https://doi.org/10.1175/1520-0450(1972)011⟨0823:CAOUEO⟩2.0.CO;2

Huff, F. A., & Changnon, S. A. (1973). Precipitation modification by major urban areas. *Bulletin of the American Meteorological Society*, *54*(12), 1220–1233. https://doi.org/10.1175/1520-0477(1973)054⟨1220:PMBMUA⟩2.0.CO;2

Istat. (2023). *Resident population on 1st January* [Dataset]. http://dati.istat.it/OECDStat_Metadata/ShowMetadata.ashx?Dataset=DCIS_POPRES1&ShowOnWeb=true&Lang=en

Jha, A. K., Bloch, R., & Lamond, J. (2012). *Cities and flooding: A guide to integrated urban flood risk management for the 21st century [Book]*. World Bank Publications. Retrieved from http://hdl.handle.net/10986/2241

Johnson, D. B. (1982). The role of giant and ultragiant aerosol particles in warm rain initiation. *Journal of the Atmospheric Sciences*, *39*(2), 448–460. https://doi.org/10.1175/1520-0469(1982)039⟨0448:TROGAU⟩2.0.CO;2

Kingfield, D. M., Calhoun, K. M., de Beurs, K. M., & Henebry, G. M. (2018). Effects of city size on thunderstorm evolution revealed through a multiradar climatology of the central United States. *Journal of Applied Meteorology and Climatology*, *57*(2), 295–317. https://doi.org/10.1175/JAMC-D-16-0341.1

Kishtawal, C. M., Niyogi, D., Tewari, M., Pielke Sr, R. A., & Shepherd, J. M. (2010). Urbanization signature in the observed heavy rainfall climatology over India. *International Journal of Climatology*, *30*(13), 1908–1916. https://doi.org/10.1002/joc.2044

Lalonde, M., Oudin, L., & Bastin, S. (2023). Urban effects on precipitation: Do the diversity of research strategies and urban characteristics preclude general conclusions? *Urban Climate*, *51*, 101605. https://doi.org/10.1016/j.uclim.2023.101605

Lemonsu, A., & Masson, V. (2002). Simulation of a summer urban breeze over Paris. *Boundary-Layer Meteorology*, *104*(3), 463–490. https://doi.org/10.1023/A:1016509614936

Li, Y., Fowler, H. J., Argüeso, D., Blenkinsop, S., Evans, J. P., Lenderink, G., et al. (2020). Strong intensification of hourly rainfall extremes by urbanization. *Geophysical Research Letters*, *47*(14), e2020GL088758. https://doi.org/10.1029/2020GL088758

Lin, Y. L., & Smith, R. B. (1986). Transient dynamics of airflow near a local heat source. *Journal of the Atmospheric Sciences*, *43*(1), 40–49. https://doi.org/10.1175/1520-0469(1986)043⟨0040:TDOANA⟩2.0.CO;2

Liu, J., & Niyogi, D. (2019). Meta-analysis of urbanization impact on rainfall modification. *Scientific Reports*, *9*(1), 7301. https://doi.org/10.1038/s41598-019-42494-2

Lochbihler, K., Lenderink, G., & Siebesma, A. P. (2017). The spatial extent of rainfall events and its relation to precipitation scaling. *Geophysical Research Letters*, *44*(16), 8629–8636. https://doi.org/10.1002/2017GL074857

Lorenz, J. M., Kronenberg, R., Bernhofer, C., & Niyogi, D. (2019). Urban rainfall modification: Observational climatology over berlin, Germany. *Journal of Geophysical Research: Atmospheres*, *124*(2), 731–746. https://doi.org/10.1029/2018JD028858

Lu, Y., Yu, Z., Albertson, J. D., Chen, H., Hu, L., Pendergrass, A., et al. (2024). Understanding the influence of urban form on the spatial pattern of precipitation. *Earth's Future*, *12*(1), e2023EF003846. https://doi.org/10.1029/2023EF003846

Marelle, L., Myhre, G., Steensen, B. M., Hodnebrog, O., Alterskjaer, K., & Sillmann, J. (2020). Urbanization in megacities increases the frequency of extreme precipitation events far more than their intensity. *Environmental Research Letters*, *15*(12), 124072. https://doi.org/10.1088/1748-9326/abcc8f

Marshall, J. D. (2007). Urban land area and population growth: A new scaling relationship for metropolitan expansion. *Urban Studies*, *44*(10), 1889–1904. https://doi.org/10.1080/00420980701471943

Met Office. (2003). 1 km resolution UK composite rainfall data from the met office nimrod system [Dataset]. *NCAS British Atmospheric Data Centre*. Retrieved from https://catalogue.ceda.ac.uk/uuid/27dd6ffba67f667a18c62de5c3456350

Mölders, N., & Olson, M. A. (2004). Impact of urban effects on precipitation in high latitudes. *Journal of Hydrometeorology*, *5*(3), 409–429. https://doi.org/10.1175/1525-7541(2004)005⟨0409:IOUEOP⟩2.0.CO;2

Moseley, C., Henneberg, O., & Haerter, J. O. (2019). A statistical model for isolated convective precipitation events. *Journal of Advances in Modeling Earth Systems*, *11*(1), 360–375. https://doi.org/10.1029/2018MS001383

Mote, T. L., Lacke, M. C., & Shepherd, J. M. (2007). Radar signatures of the urban effect on precipitation distribution: A case study for Atlanta, Georgia. *Geophysical Research Letters*, *34*(20). https://doi.org/10.1029/2007GL031903

Niyogi, D., Lei, M., Kishtawal, C., Schmid, P., & Shepherd, M. (2017). Urbanization impacts on the summer heavy rainfall climatology over the Eastern United States. *Earth Interactions*, *21*(5), 1–17. https://doi.org/10.1175/EI-D-15-0045.1

Niyogi, D., Pyle, P., Lei, M., Arya, S. P., Kishtawal, C. M., Shepherd, M., et al. (2011). Urban modification of thunderstorms: An observational storm climatology and model case study for the Indianapolis urban region. *Journal of Applied Meteorology and Climatology*, *50*(5), 1129–1144. https://doi.org/10.1175/2010JAMC1836.1

NOAA. (2023a). Multi-radar multi-sensor (MRMS) archiving [Dataset]. *Iowa Environmental Mesonet*. Retrieved from https://mtarchive.geol.iastate.edu/

Nomis. (2020). Population estimates - Small area based by single year of age - England and wales [Dataset]. https://www.nomisweb.co.uk/query/construct/summary.asp?mode=construct&version=0&dataset=2010

Ochoa-Rodriguez, S., Wang, L.-P., Gires, A., Pina, R. D., Reinoso-Rondinel, R., Bruni, G., et al. (2015). Impact of spatial and temporal resolution of rainfall inputs on urban hydrodynamic modelling outputs: A multi-catchment investigation. *Journal of Hydrology*, *531*, 389–407. https://doi.org/10.1016/j.jhydrol.2015.05.035

Oke, T. R. (1973). City size and the urban heat Island. *Atmospheric Environment*, *7*(8), 769–779. https://doi.org/10.1016/0004-6981(73)90140-6

Oke, T. R., Mills, G., Christen, A., & Voogt, J. A. (2017). *Urban climates [Book]*, Cambridge University Press. Retrieved from https://doi.org/10.1017/9781139016476

Olfe, D. B., & Lee, R. L. (1971). Linearized calculations of urban heat island convection effects. *Journal of the Atmospheric Sciences*, *28*(8), 1374–1388. https://doi.org/10.1175/1520-0469(1971)028⟨1374:LCOUHI⟩2.0.CO;2

Peleg, N., Ban, N., Gibson, M. J., Chen, A. S., Paschalis, A., Burlando, P., & Leitão, J. P. (2022). Mapping storm spatial profiles for flood impact assessments. *Advances in Water Resources*, *166*, 104258. https://doi.org/10.1016/j.advwatres.2022.104258

Peleg, N., Marra, F., Fatichi, S., Molnar, P., Morin, E., Sharma, A., & Burlando, P. (2018). Intensification of convective rain cells at warmer temperatures observed from high-resolution weather radar data. *Journal of Hydrometeorology*, *19*(4), 715–726. https://doi.org/10.1175/jhm-d-17-0158.1

Peleg, N., & Morin, E. (2012). Convective rain cells: Radar-derived spatiotemporal characteristics and synoptic patterns over the Eastern Mediterranean. *Journal of Geophysical Research*, *117*(D15). https://doi.org/10.1029/2011JD017353

Ramanathan, V., Crutzen, P. J., Kiehl, J. T., & Rosenfeld, D. (2001). Aerosols, climate, and the hydrological cycle. *Science*, *294*(5549), 2119–2124. https://doi.org/10.1126/science.1064034

Rosenfeld, D., Lohmann, U., Raga, G. B., O'Dowd, C. D., Kulmala, M., Fuzzi, S., et al. (2008). Flood or drought: How do aerosols affect precipitation? *Science*, *321*(5894), 1309–1313. https://doi.org/10.1126/science.1160606

Rotach, M. W., Vogt, R., Bernhofer, C., Batchvarova, E., Christen, A., Clappier, A., et al. (2005). Bubble – An urban boundary layer meteorology project. *Theoretical and Applied Climatology*, *81*(3), 231–261. https://doi.org/10.1007/s00704-004-0117-9

Rozalis, S., Morin, E., Yair, Y., & Price, C. (2010). Flash flood prediction using an uncalibrated hydrological model and radar rainfall data in a Mediterranean watershed under changing hydrological conditions. *Journal of Hydrology*, *394*(1), 245–255. https://doi.org/10.1016/j.jhydrol.2010.03.021

Schmid, P. E., & Niyogi, D. (2013). Impact of city size on precipitation-modifying potential. *Geophysical Research Letters*, *40*(19), 5263–5267. https://doi.org/10.1002/grl.50656

Seneviratne, S., Zhang, X., Adnan, M., Badi, W., Dereczynski, C., Di Luca, A., et al. (2021). Weather and climate extreme events in a changing climate. In V. Masson-Delmotte, et al. (Eds.), *Climate change 2021: The physical science basis. contribution of working group i to the sixth assessment report of the intergovernmental panel on climate change* (pp. 1513–1766). Cambridge University Press. https://doi.org/10.1017/9781009157896.013

Seto, K. C., Sánchez-Rodríguez, R., & Fragkias, M. (2010). The new geography of contemporary urbanization and the environment. *Annual Review of Environment and Resources*, *35*(1), 167–194. https://doi.org/10.1146/annurev-environ-100809-125336

Shastri, H., Paul, S., Ghosh, S., & Karmakar, S. (2015). Impacts of urbanization on Indian summer monsoon rainfall extremes. *Journal of Geophysical Research: Atmospheres*, *120*(2), 496–516. https://doi.org/10.1002/2014JD022061

Shepherd, J. M. (2006). Evidence of urban-induced precipitation variability in arid climate regimes. *Journal of Arid Environments*, *67*(4), 607–628. https://doi.org/10.1016/j.jaridenv.2006.03.022

Shi, T., Yang, Y., Zheng, Z., Tian, Y., Huang, Y., Lu, Y., et al. (2022). Potential urban barrier effect to alter patterns of cloud-to-ground lightning in Beijing metropolis. *Geophysical Research Letters*, *49*(21), e2022GL100081. https://doi.org/10.1029/2022GL100081

Singh, J., Karmakar, S., PaiMazumder, D., Ghosh, S., & Niyogi, D. (2020). Urbanization alters rainfall extremes over the contiguous United States. *Environmental Research Letters*, *15*(7), 074033. https://doi.org/10.1088/1748-9326/ab8980

Singh, J., Vittal, H., Karmakar, S., Ghosh, S., & Niyogi, D. (2016). Urbanization causes nonstationarity in Indian summer monsoon rainfall extremes. *Geophysical Research Letters*, *43*(21), 11–269. https://doi.org/10.1002/2016GL071238

Stewart, I. D., & Oke, T. R. (2012). Local climate zones for urban temperature studies. *Bulletin of the American Meteorological Society*, *93*(12), 1879–1900. https://doi.org/10.1175/BAMS-D-11-00019.1

Syed, K. H., Goodrich, D. C., Myers, D. E., & Sorooshian, S. (2003). Spatial characteristics of thunderstorm rainfall fields and their relation to runoff. *Journal of Hydrology*, *271*(1), 1–21. https://doi.org/10.1016/S0022-1694(02)00311-6

UN-DESA. (2018). *World urbanization prospects: The 2018 revision, online edition (Tech. Rep.)*. United Nations, Department of Economic and Social Affairs. Retrieved from https://population.un.org/wup/Download/Files/WUP2018-F01-Total_Urban_Rural.xls

Wasko, C., Sharma, A., & Westra, S. (2016). Reduced spatial extent of extreme storms at higher temperatures. *Geophysical Research Letters*, *43*(8), 4026–4032. https://doi.org/10.1002/2016GL068509

Westcott, N. E. (1995). Summertime cloud-to-ground lightning activity around major Midwestern urban areas. *Journal of Applied Meteorology*, *34*(7), 1633–1642. https://doi.org/10.1175/1520-0450-34.7.1633

Westra, S., Fowler, H. J., Evans, J. P., Alexander, L. V., Berg, P., Johnson, F., et al. (2014). Future changes to the intensity and frequency of short-duration extreme rainfall. *Reviews of Geophysics*, *52*(3), 522–555. https://doi.org/10.1002/2014RG000464

Winterrath, T., Brendel, C., Hafer, M., Junghänel, T., Klameth, A., Lengfeld, K., et al. (2018). Radklim version 2017.002: Reprocessed quasi gauge-adjusted radar data, 5-minute precipitation sums (yw) [Dataset]. *Deutscher Wetterdienst (DWD)*. https://doi.org/10.5676/DWD/RADKLIM_YW_V2017.002

Yang, L., Smith, J. A., Baeck, M. L., & Zhang, Y. (2016). Flash flooding in small urban watersheds: Storm event hydrologic response. *Water Resources Research*, *52*(6), 4571–4589. https://doi.org/10.1002/2015WR018326

Yang, L., Tian, F., & Niyogi, D. (2015). A need to revisit hydrologic responses to urbanization by incorporating the feedback on spatial rainfall patterns. *Urban Climate*, *12*, 128–140. https://doi.org/10.1016/j.uclim.2015.03.001

Yang, L., Tian, F., Smith, J. A., & Hu, H. (2014). Urban signatures in the spatial clustering of summer heavy rainfall events over the Beijing metropolitan region. *Journal of Geophysical Research: Atmospheres*, *119*(3), 1203–1217. https://doi.org/10.1002/2013JD020762

Yang, P., Ren, G., & Yan, P. (2017). Evidence for a strong association of short-duration intense rainfall with urbanization in the Beijing urban area. *Journal of Climate*, *30*(15), 5851–5870. https://doi.org/10.1175/JCLI-D-16-0671.1

Yeung, J. K., Smith, J. A., Baeck, M. L., & Villarini, G. (2015). Lagrangian analyses of rainfall structure and evolution for organized thunderstorm systems in the urban corridor of the Northeastern United States. *Journal of Hydrometeorology*, *16*(4), 1575–1595. https://doi.org/10.1175/JHM-D-14-0095.1

Zhang, J., Howard, K., Langston, C., Kaney, B., Qi, Y., Tang, L., et al. (2016). Multi-radar multi-sensor (MRMS) quantitative precipitation estimation: Initial operating capabilities. *Bulletin of the American Meteorological Society*, *97*(4), 621–638. https://doi.org/10.1175/BAMS-D-14-00174.1

Zhang, W., Yang, J., Yang, L., & Niyogi, D. (2022). Impacts of city shape on rainfall in inland and coastal environments. *Earth's Future*, *10*(5), e2022EF002654. https://doi.org/10.1029/2022EF002654

Zhang, Y., Miao, S., Dai, Y., & Bornstein, R. (2017). Numerical simulation of urban land surface effects on summer convective rainfall under different UHI intensity in Beijing. *Journal of Geophysical Research: Atmospheres*, *122*(15), 7851–7868. https://doi.org/10.1002/2017JD026614

Zhou, Z., Smith, J. A., Baeck, M. L., Wright, D. B., Smith, B. K., & Liu, S. (2021). The impact of the spatiotemporal structure of rainfall on flood frequency over a small urban watershed: An approach coupling stochastic storm transposition and hydrologic modeling. *Hydrology and Earth System Sciences*, *25*(9), 4701–4717. https://doi.org/10.5194/hess-25-4701-2021

Zhu, X., Li, D., Zhou, W., Ni, G., Cong, Z., & Sun, T. (2017). An idealized les study of urban modification of moist convection. *Quarterly Journal of the Royal Meteorological Society*, *143*(709), 3228–3243. https://doi.org/10.1002/qj.3176

References From the Supporting Information

ARPA. (2023). Dati sensori meteo [Dataset]. *ARPA*. Retrieved from https://www.arpalombardia.it/temi-ambientali/meteo-e-clima/form-richiesta-dati/

DWD. (2023). Hourly station observations of air temperature at 2 m above ground in °c for Germany, version v21.3 [Dataset]. *Climate Data Center (CDC)*. Retrieved from https://cdc.dwd.de/portal/

Met Office. (2023). MIDAS open: UK hourly weather observation data, v202308 [Dataset]. *NERC EDS Centre for Environmental Data Analysis*. https://doi.org/10.5285/c9663d0c525f4b0698f1ec4beae3688e

NOAA. (2023c). Automated surface observing system (ASOS) [Dataset]. *Iowa Environmental Mesonet*. Retrieved from https://mesonet.agron.iastate.edu/ASOS/

NOAA. (2023b). Road weather information system (RWIS) [Dataset]. *Iowa Environmental Mesonet*. Retrieved from https://mesonet.agron.iastate.edu/request/rwis/fe.phtml?network=GA_RWIS